

pH-induced metal-ligand cross-links inspired by mussel yield self-healing polymer networks with near-covalent elastic moduli

Niels Holten-Andersen^{a,1}, Matthew J. Harrington^b, Henrik Birkedal^c, Bruce P. Lee^d, Phillip B. Messersmith^d, Ka Yee C. Lee^a, and J. Herbert Waite^e

^aDepartment of Chemistry, Institute for Biophysical Dynamics, and the James Franck Institute, University of Chicago, Chicago, IL 60637; ^bDepartment of Biomaterials, Max Planck Institute for Colloids and Interfaces, Potsdam 14424, Germany; ^cDepartment of Chemistry and Interdisciplinary Nanoscience Center (iNANO), Aarhus University, Aarhus 8000, Denmark; ^dDepartment of Biomedical Engineering and Chemistry of Life Processes Institute, Northwestern University, Evanston, IL 60208; and ^eBiomolecular Science and Engineering, University of California, Santa Barbara, CA 93106

Edited* by Jacob N. Israelachvili, University of California, Santa Barbara, CA, and approved December 21, 2010 (received for review October 22, 2010)

Growing evidence supports a critical role of metal-ligand coordination in many attributes of biological materials including adhesion, self-assembly, toughness, and hardness without mineralization [Rubin DJ, Miserez A, Waite JH (2010) *Advances in Insect Physiology: Insect Integument and Color*, eds Jérôme C, Stephen JS (Academic Press, London), pp 75–133]. Coordination between Fe and catechol ligands has recently been correlated to the hardness and high extensibility of the cuticle of mussel byssal threads and proposed to endow self-healing properties [Harrington MJ, Masic A, Holten-Andersen N, Waite JH, Fratzl P (2010) *Science* 328:216–220]. Inspired by the pH jump experienced by proteins during maturation of a mussel byssus secretion, we have developed a simple method to control catechol-Fe³⁺ interpolymer cross-linking via pH. The resonance Raman signature of catechol-Fe³⁺ cross-linked polymer gels at high pH was similar to that from native mussel thread cuticle and the gels displayed elastic moduli (G') that approach covalently cross-linked gels as well as self-healing properties.

biomaterials | catecholate polymer | metal coordination | reversible cross-links | physical gels

Mussel byssal threads are protected against wear by a cuticle, an outer proteinaceous coating, that despite a hardness of ~0.1 GPa, accommodates large cyclic strains in the turbulent intertidal zone (1, 2). During strain, the cuticle suppresses macroscale failure by limiting crack propagation to the microscale (1, 3). It was recently demonstrated that a small amount of Fe (<1 wt%) plays an important role in this mechanism; bonding with the catechol-like amino acid dihydroxy-phenylalanine (dopa) in the cuticle protein, mfp-1 (4–6). Tris- and bis-catechol-Fe³⁺ complexes possess some of the highest known stability constants of metal-ligand chelates ($\log K_S \approx 37\text{--}40$, where K_S is the equilibrium constant for the complex formation) (7–10) and single molecule tensile tests have demonstrated that the breaking of a metal-dopa bond requires a force only modestly lower than the force required to rupture a covalent bond under identical loading conditions (~0.8 nN vs. ~2 nN, respectively) (11). Harrington et al. proposed a model where the catechol-Fe³⁺ complexes in the cuticle function as sacrificial load-bearing cross-links facilitating extensibility of the material (4). In contrast to covalent bonds, metal-dopa bonds can spontaneously reform after breaking (11) and the model predicts that the damage accumulated in the cuticle could self-heal via reformation of broken catechol-Fe³⁺ complexes (4). Here we describe a strategy for introducing bis- and/or tris-catechol-Fe³⁺ cross-links into a synthetic polymer network and demonstrate that such a network indeed displays high elastic moduli and self-healing properties.

Results

The stoichiometry of catechol-Fe³⁺ complexes (mono-, bis-, or tris-) is controlled by pH via the deprotonation of the catechol

hydroxyls (Fig. 1A). The pH required to establish the bis- and tris-complexes is typically reported to be above pH 7 (7, 8, 10), however, the solubility of Fe³⁺ is very low at anything but acidic pH (at pH 7, only 10⁻¹⁸ M aqueous Fe³⁺ is present in solution) (12). To our knowledge, this obstacle is one of the primary reasons that no condensed material other than the mussel thread cuticle and adhesive has been established via Fe³⁺-catechol cross-links above pH 7 (5, 7, 9, 13, 14). By mimicking the mussel's own process for byssus formation, we have overcome this difficulty and devised an original method with which to form catechol-Fe³⁺ polymer cross-links at basic pH that avoids Fe³⁺ precipitation.

Byssal threads self-assemble in the ventral groove of the mussel foot upon secretion of preassembled thread materials from intracellular granules of byssal gland cells (15). The byssus secretion has recently been proposed to be acidic (pH ~5–6) (16) and will be more fully described elsewhere. We propose that Fe³⁺ is prebound in mono-dopa-Fe³⁺ complexes by mfp-1 in secretory granules at pH ≤ 5. Upon release into seawater (pH ~8), the significant pH jump would cause nascent thread cuticle material to undergo a spontaneous cross-linking via bis- and/or tris-dopa-Fe³⁺ complexes (see Fig. 1B for schematic). To test this mechanism of pH-controlled cross-linking we used a simple dopa-modified polyethylene glycol polymer (PEG-dopa₄, Fig. 2A). We first verified the stoichiometric transitions of the catechol-Fe³⁺ complexes expected with increasing pH by reacting dilute PEG-dopa₄ with FeCl₃ in a dopa:Fe molar ratio of 3:1 (Fig. S1). The initially green solution turned blue and finally red as the catechol-Fe³⁺ stoichiometry changed from mono- to bis- to tris-, respectively. Identical shifts in absorbance have been reported elsewhere (17). The relative fractions of the three coordination states, extracted from the absorbance data (see *Methods* for details), show that the monospecies dominate at pH < 5.6, bis- at 5.6 < pH < 9.1, and tris- at pH > 9.1 (Fig. 2B). We next tested the effect of catechol-Fe³⁺ cross-linking on concentrated polymer networks (dopa:Fe 3:1) at pH ~5 (proposed pH of secretory granules), pH ~8 (pH of seawater), and pH ~12 (complete tris-catechol-Fe³⁺ cross-linking). Employing our mussel-inspired method of prebinding Fe³⁺ in mono-catechol-Fe³⁺ complexes at acidic pH successfully prevents ferric hydroxide precipitation

Author contributions: N.H.-A., P.B.M., K.Y.C.L., and J.H.W. designed research; N.H.-A., M.J.H., H.B., and J.H.W. performed research; B.P.L. and P.B.M. contributed new reagents/analytic tools; N.H.-A., M.J.H., H.B., P.B.M., K.Y.C.L., and J.H.W. analyzed data; and N.H.-A., M.J.H., H.B., P.B.M., K.Y.C.L., and J.H.W. wrote the paper.

Conflict of interest statement: The authors declare no competing financial interests but a patent application has been filed on this work.

*This Direct Submission article had a prearranged editor.

¹To whom correspondence should be addressed. E-mail: holten@uchicago.edu.

This article contains supporting information online at www.pnas.org/lookup/suppl/doi:10.1073/pnas.1015862108/-DCSupplemental.

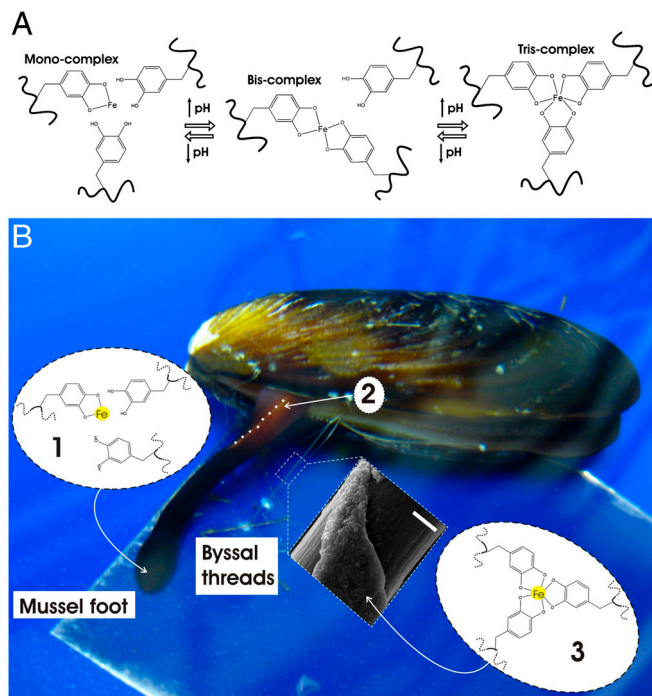


Fig. 1. Mussel-inspired Dopa-Fe³⁺ cross-linking. (A) The pH-dependent stoichiometry of Fe³⁺-catechol complexes. (B) Schematic of proposed cross-linking mechanism of byssal thread cuticle: (i) Production and storage of mfp-1 and Fe³⁺ in specialized cells of the epithelium lining the ventral groove of the mussel foot. Low pH (≤ 5) ensures mono-catechol-Fe³⁺ complexes (no cross-linking), (ii) Secretion and self-assembly of cuticle with whole mussel thread in the ventral groove (outline of part of ventral groove indicated with dashed white line), (iii) Seawater exposure (pH ~ 8) of nascent byssal thread drives immediate cuticle cross-linking via bis- and/or tris-catechol-Fe³⁺ complexes (insert shows scanning electron micrograph of mussel thread with partial cuticle on top of fibrous core) (Scale bar, 20 μm).

when raising pH to initiate cross-linking. The concentrated polymer-FeCl₃ mixture remained a green/blue fluid upon raising pH to ~ 5 , whereas raising pH to ~ 8 resulted in the instant formation of a sticky purple gel. At pH ~ 12 a red elastomeric gel immediately formed (Fig. 2C and Fig. S2 A-C, G, I, and Movie S1). UV-Vis absorbance spectroscopy confirmed the dominance of mono-, bis-, and tris-catechol-Fe³⁺ complexes, in the pH ~ 5 , ~ 8 , and ~ 12 adjusted polymer networks, respectively (Fig. S1). Raman microspectroscopy performed with a near-infrared (785 nm) laser furthermore demonstrated resonance Raman spectra characteristic of Fe³⁺-catechol coordination in the polymer networks after FeCl₃ was added (Fig. 2D). Clear spectral differences exist between samples, particularly in the Raman band originating specifically from the chelation of the Fe³⁺ ion by the oxygen atoms of the catechol (470–670 cm⁻¹). This band consists of three major peaks, which transform significantly with changing pH. The peaks at ~ 590 cm⁻¹ and ~ 633 cm⁻¹ are assigned to the interaction between the Fe³⁺ ion and the C₃ and C₄ oxygens of the catechol, respectively, while the peak at 528 cm⁻¹ is assigned to charge transfer (CT) interactions of the bidentate chelate (see Fig. 1A) (18). The area of the CT peak increases relative to the other two peaks upon increasing pH from about 6% at pH ~ 5 to $\sim 30\%$ at pH ~ 8 and almost 40% at pH ~ 12 . This peak progression suggests an increase in bidentate complexation with increasing pH consistent with the transition from mono- to tris-coordinated Fe³⁺ species. Moreover, the resonance signals from the tris-catechol-Fe³⁺ cross-linked gels at pH ~ 12 and reconstituted Fe³⁺ mfp-1 complexes (7) were found to be remarkably similar to the native mussel thread cuticle (Table S1 and Fig. 2D) (4).

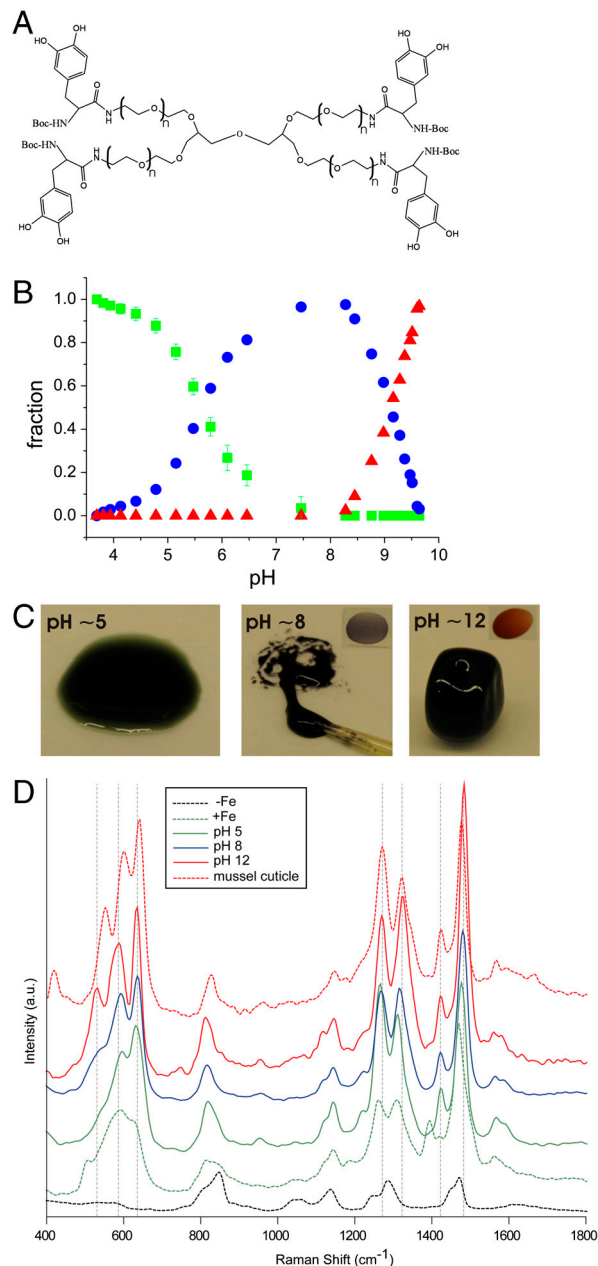


Fig. 2. PEG-dopa₄-Fe³⁺ crosslinking. (A) Dopa-modified polyethylene glycol (PEG-dopa₄, 10 kDa PEG core). (B) Relative fractions of mono- (green), bis- (blue), and tris-catechol-Fe³⁺ (red) complexes in solutions of PEG-dopa₄ with FeCl₃ at a dopa:Fe molar ratio of 3:1 as a function of pH. (C) Physical state and color of PEG-dopa₄ gels in mono- (green/blue), bis- (purple), and tris-catechol-Fe³⁺ (red) complexation (dopa:Fe 3:1). Insets highlight color of bis- and tris-catechol-Fe³⁺ cross-linked gels. (D) Resonance Raman spectroscopy of the same samples as in (C). Spectra of PEG-dopa₄ without (dashed black) and with (dashed green) FeCl₃ (unadjusted pH ~ 3 –4) are shown for comparison. Additionally, the spectrum from the native mussel thread cuticle is included (dashed red). For each spectra $N = 3$.

In agreement with their lack of cross-linking, concentrated polymer-FeCl₃ mixtures at pH ~ 5 displayed a viscous response in dynamic oscillatory rheology, whereas the bis- and tris-catechol-Fe³⁺ cross-linked gels at pH ~ 8 and pH ~ 12 , respectively, behaved increasingly elastically (elastic modulus G' > viscous modulus G'') (Fig. 3A). For comparison, a covalently cross-linked polymer gel was prepared using NaIO₄-induced oxidation of PEG-dopa₄ (19) (Fig. S2 D–H). When a tris-catechol-Fe³⁺ cross-linked gel and a covalent gel were exposed to a concentrated

Additionally, the tris-catechol-Fe³⁺ cross-linked gels reestablish their stiffness and cohesiveness within minutes after failure (see Fig. 3C) likely through restoration of broken catecholato-Fe³⁺ cross-links analogous to what has been observed in other types of reversible polymer networks with weaker noncovalent cross-links such as ionic and hydrogen bonds (22, 23). The effects of polymer size, cross-link density, and Fe:dopa ratio on the relaxation and self-healing time of catecholato-Fe³⁺ cross-linked polymer networks are currently under investigation.

Although the relevance of our findings to byssus formation remains tentative at this time, to a first approximation, we have measured the effect of the proposed pH jump from secretory granules to seawater on catecholato-Fe³⁺ cross-linked polymer networks. The overall similarity of the resonance signals from tris-catechol-Fe³⁺ cross-linked gels and reconstituted Fe³⁺ mfp-1 with native mussel thread cuticle (see Table S1 and Fig. 2D) supports that tris-dopa-Fe³⁺ complexes cross-link mfp-1 in the natural coating. However, the Raman signature of the mussel thread cuticle is more similar to gels cross-linked at pH ~ 12 than at the pH of seawater and small differences were found between tris-catechol-Fe³⁺ cross-linked gels and cuticle. These disparities likely arise from differences in the microenvironment and conformation between mfp-1 protein in the native thread cuticle and our *in vitro* polymer scaffolds.

The viscoelastic properties that arise from catecholato-Fe³⁺ cross-links in polymeric networks could be advantageous to the mussel in the following ways. A concentrated secretion of mfp-1, weakly cross-linked with low levels of bis-dopa-Fe³⁺ complexes initially, could provide ideal properties for coating deposition as a viscous fluid similar to what has been proposed for the underwater sandcastle glue of *Phragmatopoma californica* (24). Once fully exposed to ocean pH, during periods of strong wave action with fast flows, the high stiffness of a tris-dopa-Fe³⁺ cross-linked mfp-1 scaffold, combined with its capacity to yield before covalent failure of the protein backbone, would offer ideal protection of the mussel thread. Periods of low wave action could subsequently allow the microdamage developed in the cuticle to self-heal.

These adaptive properties of the thread coating would not only have value to mussels but to engineers as well and in contrast to the mussel adhesive proteins, PEG-dopa polymers are not limited to iron as the cross-linking metal. Dopa has high affinities for other metals, and we have preliminary data illustrating that titanium ions result in the formation of gels with different viscoelastic properties (Fig. S4). The distinct chemical properties of the coordination complexes between PEG-dopa and different metals, including possible covalent cross-linking induced by varying metal redox activities, expand the range of accessible synthetic material properties and are currently under investigation. Furthermore, other metal-coordinating ligands than catechols, could be envisaged to decorate PEG or other types of water soluble polymer backbones with desirable properties and applied in pH-controlled polymer cross-linking following our protocol. In general, cross-linking of polymer networks by metal-ligand coordination has manifold advantages: (i) Relative to covalent cross-linking, metal-ligand coordination offers the promise of materials with comparable strength plus intrinsic self-healing. (ii) Vis-à-vis other reversibly cross-linked polymer networks based on electrostatic, H-bond, or hydrophobic interactions (25–27), cross-linking based on multiple ligand-metal complexes such as metal-catecholates offers near covalent stabilities with noncovalent reformation rates and a range of possible cross-link modes from zero to three per metal ion. (iii) While the metal-ligand-complex theme can also be utilized to cross-link polymers in organic solvents (28) its incorporation into polymers in aqueous solvents under ambient conditions by simply increasing pH as presented here, provides a unique promising platform for environmental and physiological applications. (iv) Finally,

in our initial polymer system, the pH-tunable cross-link kinetics offer easy control of viscoelastic properties over four orders of magnitude in modulus, from a low viscosity fluid to a stable self-healing gel. Adhesives and coatings based on PEG-dopa are already recognized to impart substantial advantages for applications in dry and wet environments (29, 30). Our findings significantly amplify the scope of these.

Methods

Synthesis of PEG-(N-Boc-dopa)₄. Polymer was synthesized as described in Lee et al. (19). Briefly, 4-arm-PEG-amine [PEG-(NH₂)₄, *M_w* = 10,000] was purchased from SunBio, Inc. PEG-(NH₂)₄ (6.0 g, 0.60 mmol) was reacted with N-Boc (butoxycarbonyl)-L-DOPA dicyclohexylammonium salt (4.8 mmol), HOBt (1-Hydroxybenzotriazole) (8.0 mmol), and Et₃N (8.0 mmol) in 60 mL of a 50:50 mixture of dichloromethane and dimethylformamide. HBTU [2-(1h-benzotriazol-1-yl)-1,1,3,3-tetramethyluronium hexafluorophosphate] (4.8 mmol) in 30 mL of dichloromethane was then added, and the coupling reaction was carried out under argon at room temperature for 1 h. The solution was successively washed with saturated sodium chloride solution, 5% NaHCO₃, diluted HCl solution, and distilled water. The crude product was concentrated under reduced pressure and purified by column chromatography on Sephadex LH-20 with methanol as the mobile phase. The product was further purified by precipitation in cold methanol three times, dried in a vacuum at room temperature, and stored under nitrogen at –20 °C. Gel permeation chromatography-multiple-angle laser light scattering revealed an increase in polymer molecular weight of ~1,400 compared to the starting material in agreement with addition of four butoxycarbonyl-dopa groups.

Fe³⁺-Catechol Cross-Linked Gels. The above described PEG-(N-Boc-dopa)₄ was used for all gel experiments. Freeze-dried aliquots of the polymer stored under Argon or N₂ at –20 °C, were equilibrated to room temperature for 1 h before opening sample vial to prevent water condensation on the sample. A typical 400 μL Fe³⁺-catechol cross-linked gel was made as follows: **1)** 200 μL of polymer solution was prepared by dissolving 40 mg polymer in unbuffered Milli-Q water to a starting concentration of 200 mg/mL (corresponds to a dopa concentration of 80 mM). **2)** The polymer solution was mixed with 1/6 final volume (66.7 μL) of 80 mM (13 mg/mL) FeCl₃ (Sigma). A green color developed immediately upon mixing (see Fig. S2A). **3)** The gel was established by adding 2/6 final volume (133.3 μL) of NaOH (Sigma) at a concentration adjusted to induce the desired final pH of the gel. This resulted in instant gelation and color development according to gel pH (see Fig. S2B). **4)** The gel was physically mixed until a homogenous color and physical state were established (~60 s). A short movie that illustrates the gel formation is available (see Movie S1). Samples were tested in rheology immediately after mixing, except for gels compared to covalent gels which were then sealed in airtight containers to prevent dehydration (~6 h cure time). The final concentration of PEG-(N-Boc-dopa)₄ in all gels was thereby 100 mg/mL (10 wt%) with a final molar ratio of dopa to FeCl₃ of 40 to 13.3 mM (3:1). This corresponds to 0.74 mg/mL (0.074 wt%) of Fe. We established samples at a final pH ~ 5 (predominantly mono-catecholato-Fe³⁺ complexes at the proposed pH of secretory granules), pH ~ 8 (predominantly bis-catecholato-Fe³⁺ cross-links at the pH of seawater), and pH ~ 12 (pure tris-catecholato-Fe³⁺ cross-links). The pH of gels was measured using a pH-meter with a flat surface electrode designed for solids, semisolids, and liquids (FieldScout SoilStik pH Meter, Spectrum Technologies).

Ti-Cross-Linked Gels. The above protocol for formation of Fe³⁺-catechol cross-linked PEG-dopa₄ gels was followed substituting FeCl₃ with TiCl₃ (Sigma) using a total of 6 M equivalents of NaOH when inducing the cross-linking.

Covalently Cross-Linked Gels. These gels were established by mixing 200 mg/mL polymer solution with an equal volume of 40 mM (8.6 mg/mL) NaIO₄ (dopa: IO₄⁻ molar ratio of 2:1) (Sigma) which resulted in immediate orange color development and slow gelation (see Fig. S2 D and E). The covalent gels needed to be precast before they cured due to the elastic nature of the final gel material. Immediately after casting, the samples were sealed in airtight containers until rheology testing (~6 h cure time), except for tests of cross-linking rate where an enclosed test cell served to avoid sample dehydration.

Rheology of Gels. The mechanical properties of the hydrogels were tested using a rheometer (Anton Paar) with parallel plate geometry (25 mm or 50 mm diameter rotating top plate). All tests (except for tests of the rate

of cross-linking) were done immediately after transferring the gel sample onto the sample stage. Oscillatory shear testing of gels as a function of frequency was performed at constant 10 mrad strain (~20% strain, linear viscoelastic regime 0~60% strain) while measuring storage modulus (G') and loss modulus (G''). Recovery tests were performed by straining each gel to failure under increasing oscillations to 1,000 mrad immediately followed by linear conditions (1% strain, 1 Hz) while monitoring the recovery of the storage modulus (G'). For both types of gels, G' was normalized to values in the linear regime to allow easier comparison. Water loss during testing was negligible due to typical gap distances between parallel plates of ~0.4 mm and typical test time of <30 min. During longer measurements of the rates of cross-linking, the tests were performed in an enclosed cell as a precaution to avoid sample dehydration. All tests were performed at 20 °C. Data points that represents measurements of G' of the pH 5 sample have been removed from the plot in Fig. 3A due to excessive interference from equipment resonance on samples with such low elasticity.

Absorbance Spectrophotometry. The dopa- Fe^{3+} cross-linking stoichiometry and the dopa oxidation were monitored on a UV-visible light spectrophotometer (Perkin Elmer) using a quartz cuvette with a path length of 1 cm. Spectral changes of solutions of 1 mg/mL PEG-dopa₄ (0.4 mM_{dopa}) with 22 $\mu\text{g/mL}$ (0.13 mM) FeCl_3 (dopa:Fe molar ratio of 3:1) were followed while increasing pH with 1 M NaOH up to a final pH ~10. The absorbance of 4 mg/mL PEG-dopa₄ (1.6 mM_{dopa}) with 4.3 mg/mL (0.8 mM) NaIO_4 (dopa: IO_4^- molar ratio of 2:1) was monitored immediately following mixing. Furthermore, the absorbance of 4 mg/mL PEG-dopa₄ with 88 $\mu\text{g/mL}$ FeCl_3 (dopa:Fe 3:1) before and after increasing pH from ~3 to ~9 was recorded for comparison with the NaIO_4 induced spectral changes. Absorbance of gels was measured holding the gel between two cover slips and placing them directly in the light path of the spectrophotometer.

To extract the relative abundance of the three dopa- Fe^{3+} cross-linking species, the UV/VIS absorbance data from Fig. S1 were fitted to peak functions in an iterative manner to obtain spectra of the three species that could be used to fit all spectra. For quantification, only the peaks above 400 nm were used because the data below this range were too severely affected by overlap; the main absorption above 400 nm of the monospecies was found to be a doublet at 406 and 759 nm, the dimer had a peak at 575 nm while the trimer had a peak at 492 nm. These values agree with spectra reported in the literature for similar species (9, 10, 31). The areas of the peaks were then normalized to the maximum value for each peak. No constraints on the sum

of the fractions were imposed during the fitting procedure. Gratifyingly, the largest deviation from unity was 3.4 estimated standard deviations (esd) with an average of 1.6 esd indicating that the fits successfully distributed the intensity into the respective contributions. The data shown in Fig. 2B have been normalized so that the sum of the mole fractions is equal to one.

Resonance Raman Spectroscopy. For Raman spectroscopic studies, a continuous laser beam was focused on the samples through a confocal Raman microscope (CRM200, WITec) equipped with a piezo-scanner (P-500, Physik Instrumente). The diode-pumped 785 nm near infrared laser excitation (Toptica Photonics AG) was used in combination with a 20 \times microscope objective (Nikon, NA = 0.4). The spectra were acquired using an air-cooled CCD (DU401A-DR-DD, Andor) behind a grating (300 gmm^{-1}) spectrograph (Acton, Princeton Instruments Inc.) with a spectral resolution of 6 cm^{-1} . Because the samples were sensitive to burning by the laser beam, a laser power of between 10–20 mW, combined with a short integration time of 0.2 s was used for all measurements. The ScanCtrlSpectroscopyPlus software (version 1.38, Witec) was used for measurement setup and spectral processing. Each collected spectra consisted of 60 accumulations of a 0.2 s integration time. For each sample, three spectra were collected from different regions and averaged. Averaged spectra were smoothed with a Savitzky-Golay smoothing filter, and a second order polynomial background was subtracted from the smoothed spectra (4, 7, 32, 33).

ACKNOWLEDGMENTS. The authors thank Professors Tom Witten, Margaret Gardel, and Dr. Eric Brown (University of Chicago) for valuable discussions of the manuscript, insights on the rheological properties of the gels, and assistance with the experimental set-up. We thank Professor Heinrich Jaeger (University of Chicago) for the use of the rheometer and Tara J. Fadenrecht for shooting and editing the video of the formation of the high pH PEG-dopa₄ Fe-gel. N.H.A. and H.B. thank the Danish Council for Independent Research | Natural Sciences for funding. M.J.H. was partially funded by an Alexander von Humboldt Research Fellowship for Postdoctoral Researchers. This work was supported by the National Science Foundation (NSF) Materials Research and Engineering Centers (MRSEC) Program at the University of Chicago (DMR-0820054), and National Institutes of Health (NIH) grants to J.H.W. (R01DE018468) and P.B.M. (R37DE014193 and RC1DE020702), and NSF grant to K.Y.C.L. (MCB-0920316). We acknowledge MRSEC Shared Facilities (University of Chicago) and the Biophysical Core Facility (University of Chicago) for the use of their instruments.

- Holten-Andersen N, Fantner GE, Hohlbauch S, Waite JH, Zok FW (2007) Protective coatings on extensible biofibers. *Nat Mater* 6:669–672.
- Rubin DJ, Miserez A, Waite JH (2010) *Advances in insect physiology: insect integument and color*, eds C Jérôme and JS Stephen (Academic Press, London), pp 75–133.
- Holten-Andersen N, Zhao H, Waite JH (2009) Stiff coatings on compliant biofibers: the cuticle of *Mytilus californianus* byssal threads. *Biochemistry* 48:2752–2759.
- Harrington MJ, Masic A, Holten-Andersen N, Waite JH, Fratzl P (2010) Iron-clad fibers: a metal-based biological strategy for hard flexible coatings. *Science* 328:216–220.
- Zeng H, Hwang DS, Israelachvili JN, Waite JH (2010) Strong reversible Fe^{3+} -mediated bridging between dopa-containing protein films in water. *Proc Natl Acad Sci USA* 107:12850–12853.
- Holten-Andersen N, et al. (2009) Metals and the integrity of a biological coating: the cuticle of mussel byssus. *Langmuir* 25:3323–3326.
- Taylor SW, Chase DB, Emptage MH, Nelson MJ, Waite JH (1996) Ferric ion complexes of a dopa-containing adhesive protein from *Mytilus edulis*. *Inorg Chem* 35:7572–7577.
- Taylor SW, Luther GW, Waite JH (1994) Polarographic and spectrophotometric investigation of iron(III) complexation to 3,4-Dihydroxyphenylalanine-containing peptides and proteins from *Mytilus-Edulis*. *Inorg Chem* 33:5819–5824.
- Sever MJ, Weisser JT, Monahan J, Srinivasan S, Wilker JJ (2004) Metal-mediated cross-linking in the generation of a marine-mussel adhesive. *Angewandte Chemie International Edition* 43:448–450.
- Avdeef A, Sofen SR, Bregante TL, Raymond KN (1978) Coordination chemistry of microbial iron transport compounds. 9. Stability constants for catechol models of enterobactin. *J Am Chem Soc* 100:5362–5370.
- Lee H, Scherer NF, Messersmith PB (2006) Single-molecule mechanics of mussel adhesion. *Proc Natl Acad Sci USA* 103:12999–13003.
- Butler A (1998) Acquisition and utilization of transition metal ions by marine organisms. *Science* 281:207–209.
- Loizou E, et al. (2006) Structural effects of cross-linking a biopolymer hydrogel derived from marine mussel adhesive protein. *Macromol Biosci* 6:711–718.
- Hwang DS, et al. (2010) Protein- and metal-dependent interactions of a prominent protein in mussel adhesive plaques. *J Biol Chem* 285:25850–25858.
- Zuccarello LV (1981) Ultrastructural and cytochemical study on the enzyme gland of the foot of a mollusc. *Tissue Cell* 13:701–713.
- Zhao H, Waite JH (2006) Linking adhesive and structural proteins in the attachment plaque of *Mytilus californianus*. *J Biol Chem* 281:26150–26158.
- Sever MJ, Wilker JJ (2006) Absorption spectroscopy and binding constants for first-row transition metal complexes of a dopa-containing peptide. *Dalton Transactions* 6:813–822.
- Michaud-Soret I, et al. (1995) Resonance Raman studies of catecholate and phenolate complexes of recombinant human tyrosine hydroxylase. *Biochemistry* 34:5504–5510.
- Lee BP, Dalsin JL, Messersmith PB (2002) Synthesis and gelation of dopa-modified poly(ethylene glycol) hydrogels. *Biomacromolecules* 3:1038–1047.
- Roberts MC, Hanson MC, Massey AP, Karren EA, Kiser PF (2007) Dynamically restructuring hydrogel networks formed with reversible covalent crosslinks. *Adv Mater* 19:2503–2507.
- Lieleo O, Claessens MMAE, Luan Y, Bausch AR (2008) Transient binding and dissipation in cross-linked actin networks. *Phys Rev Lett* 101:108101.
- Ewoldt RH, Clasen C, Hosoi AE, McKinley GH (2007) Rheological fingerprinting of gastropod pedal mucus and synthetic complex fluids for biomimicking adhesive locomotion. *Soft Matter* 3:634–643.
- Skrzeszewska PJ, et al. (2010) Fracture and self-healing in a well-defined self-assembled polymer network. *Macromolecules* 43:3542–3548.
- Shao H, Stewart RJ (2010) Biomimetic underwater adhesives with environmentally triggered setting mechanisms. *Adv Mater* 22:729–733.
- Pezron E, et al. (1988) Reversible gel formation induced by ion complexation. 1. Borax-galactomannan interactions. *Macromolecules* 21:1121–1125.
- Kushner AM, et al. (2009) A biomimetic modular polymer with tough and adaptive properties. *J Am Chem Soc* 131:8766–8768.
- Serero Y, et al. (1998) Associating polymers: from “flowers” to transient networks. *Phys Rev Lett* 81:5584–5587.
- Kersey FR, Loveless DM, Craig SL (2007) A hybrid polymer gel with controlled rates of cross-link rupture and self-repair. *J R Soc Interface* 4:373–380.
- Lee H, Lee BP, Messersmith PB (2007) A reversible wet/dry adhesive inspired by mussels and geckos. *Nature* 448:338–341.
- Lee H, Dellatore SM, Miller WM, Messersmith PB (2007) Mussel-inspired surface chemistry for multifunctional coatings. *Science* 318:426–430.
- Crisponi G, Nurchi VM, Pivetta T (2008) Potentiometric and spectrophotometric equilibrium study on Fe(III) and new catechol-bisphosphonate conjugates. *J Inorg Biochem* 102:209–215.
- Andersson KK, Cox DD, Que L, Flatmark T, Haavik J (1988) Resonance Raman studies on the blue-green-colored bovine adrenal tyrosine 3-monooxygenase (tyrosine hydroxylase). Evidence that the feedback inhibitors adrenaline and noradrenaline are coordinated to iron. *J Biol Chem* 263:18621–18626.
- Andersson KK, et al. (1992) Purification and characterization of the blue green rat pheochromocytoma-(PC12) tyrosine-hydroxylase with a dopamine-Fe(III) complex—reversal of the endogenous feedback inhibition by phosphorylation of serine-40. *Biochem J* 284:687–695.